Model Driven Optimization of Drug Delivery for Spinal Cord Injury

A Thesis

Submitted to the Faculty

of

Drexel University

by

Neil Mittal

in Partial Fulfillment of the

Requirements for the Degree

of

Master's in Science

in

Biomedical Engineering: Tissue Engineering and Biomaterials

June, 2017

Acknowledgements

First thanks to my advisor, Yinghui Zhong, and the rest of her lab group, for their patience and the guidance I received in my first foray into academic research (Bob, Zhicheng, you have the patience of mountains). Also, I'd like to express my gratitude to my committee, Frank Ji and Lin Han, for their input and patience, right until the last second.

Next, special thanks to those who have made my final project possible with their help along the way without being official collaborators. Fred Allen, Jay Bhatt, Joseph Sarver, Boris Polyak, Hugo Woerdeman, DJ Hall, Alexander Nikolaev, Daryl Falco, Jaimie Dougherty, have all at one point or another lent their expertise or guidance, or their connections. Please forgive me if I missed anyone!

Thanks to the Drexel Biomedical Engineering Department and advising staff. Laurie, you're almost done answering emails from me with questions I should already be able to answer.

Thanks to my friends, classmates, and above all, my family and incredibly supportive partner, Kathryn, for listening me throw math and science ideas at them late night after late night. (Hi, Mom! I did it!)

Table of Contents

List of Tables

List of Figures

Terms and Abbreviations

DS: Dextran Sulfate

MH: Minocycline Hydrochloride

Mg^{2+}: Magnesium Divalent Cations

MVC: Motor Vehicle Collision

ADL: Activities of Daily Living

CNS: Central Nervous System

SCI: Spinal Cord Injury

TSCI: Traumatic Spinal Cord Injury

Abstract

Model Driven Optimization of Drug Delivery for Spinal Cord Injury
Neil Mittal, MD
Advisor: Yinghui Zhong, Ph.D

Spinal cord injuries have an annual new case incidence in the United States of up to 40 cases per million population, with a 36.2% 10 year survival rate in patients over 50 years old. Barely half of survivors from 40 to 60 can perform activities of daily living, regardless of the severity of the initial injury. [1] Spinal cord injury is progressive, mediated by secondary injury, or a subacute inflammatory process that is poorly understood. [2-4] Secondary injury can involve or lead to apoptosis, scarring, cavitation, ischemia, and demyelination, among other sequelae, and many of these are not conducive to neuronal recovery. [4] Therefore there is a need for improved ways of addressing secondary injury mechanisms in these patients. [2]

Minocycline can target multiple secondary injury mechanisms through its anti-inflammatory, anti-oxidative, and anti-apoptotic effects. [5-7] However, it is only fully effective at high concentrations. At the systemic levels required for this, minocycline can cause liver toxicity and even death. [8] Minocycline can form self-assembling, water insoluble particles with dextran sulfate and divalent metal cations, with high entrapment efficiency and a stable, slow release. There is potential for a controllable vehicle for drug delivery to optimize dosing with minocycline. [8]

Predicting minocycline release behavior of a complex system can be performed by the creation of a model to simplify the system to an equation. This simplification can be

guided by a combination of theoretical frameworks and previous empirical data that suggests idealized ratios between the components; previous work suggests the highest entrapment efficiency given a 1.2:1 mass concentration ratio of dextran sulfate:minocycline, in the presence of 7.2 mM Mg^{2+}, suggesting saturation of binding sites at these values. [8] With a high degree of accuracy, this model can help direct the optimization of the drug delivery system. In the case of minocycline:dextran sulfate:Mg^{2+}, the model proposed in this study was able to predict the trend of behavior but not with enough sensitivity for small dosing changes that characterize this delivery method.

Biomedical engineering is an interdisciplinary field that combines understanding of various scientific and design expertise. In order to tailor a drug delivery system, as well as help to characterize the mechanism of release, generating a simple model can provide insight to the behavior of the system while reducing time, labor, and cost.

Introduction

Problem Background

Spinal Cord Injury

Spinal cord injuries (SCI) occur with an estimated incidence of 12,000 new cases annually in the United States. The median age of occurrence is 36.9 years old as of 2010, with a higher male incidence, though increased survival results in a greater female prevalence. There is a lower incidence outside of the United States that is attributed to lower survival rates of causational events. Survival of the spinal insult has been shown to decrease over time after injury. [1]

The most common cause of traumatic spinal cord injuries (TSCI) is reported to be motor vehicle collision (MVC), causing 48.3% of TSCI cases. For the over 60 year old population, falls are the leading cause. The 10 year survival rate patients injured at age 50 is 36.2%, but only 56.2% of patients between the ages of 40 and 60 can perform their activities of daily living (ADL) for functional independence, regardless of injury severity. This percentage decreases with age. [1] There has been little change in survival rate since the year 2000 for cervical spinal injury. The population of SCI survivors included 48% cervical injury, a number that has remained stable due to the high mortality of these injuries. [1]

In the Major Trauma Outcomes Study, performed in North America from 1982-1989, MVC was also shown as the most common cause of TSCI and a high predilection for cervical injury (over 50% in all cases, up to 65% in cases of isolated injury). Of all trauma patients admitted, 2.6% had TSCI, and of these there was an average 17% mortality across all TSCI cases. [9] SCI is characterized not only by the initial insult, but

also by an evolving, subacute, progressive secondary injury that is well documented but still poorly understood. [2-4]

SCI therefore carries a high risk of a loss of functional independence, with profound effects on mobility, sensation, and the health of innervated tissues. SCI can cause chronic pain, paresthesias, and disability. [10]

Secondary Injury

Secondary injury is a progressive state of chronic tissue damage that persists after the initial injury. It can be much larger than the acute phase injury, with broader effects (see Figure 1). [10] Secondary injury is caused by hemorrhage, oxidative stress, glutamate toxicity, and excitotoxicity. [10] Secondary injury progression can take a variety of forms including apoptosis, scar formation, cavitation or cyst formation, demyelination, energy failure, inflammation, local toxicity or excitotoxicity, ischemia, reperfusion injury, and oxidative stresses. [4, 10]

The major inducers of secondary injury are instigated by the initial insult and inflammatory processes. [10] It directly causes apoptosis, demyelination, and tissue loss or cavitation. Treatment is not reliable, and the remaining tissue mass correlates to remaining functionality. [10]

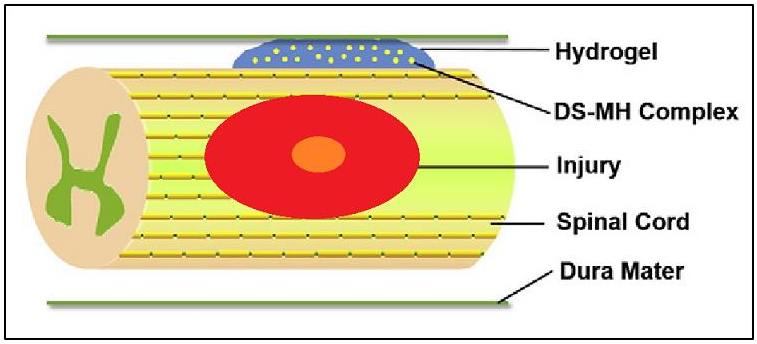

Figure 1: Secondary injury, in red, progresses beyond initial tissue insult, in orange

Z. Wang, et al. "Local delivery of minocycline from metal ion-assisted self-assembled complexes promotes neuroprotection and functional recovery after spinal cord injury", Biomaterials, vol. 112, pp. 62-71, 2017.

Secondary injury can progress beyond the initial tissue insult (see Figure 1), and has been shown to result in the formation of cysts and progressive cavitary lesions. [3] This progression follows the inflammatory response that is a consequence of traumatic injury; post traumatic cavitation is preventable but dangerous and clinically significant as a sequela of TSCI in up to 3% of cases regardless of severity of the initial injury. [2, 3] Therapeutic approaches are few and non-standardized, with surgical and shunting methods being the most favorable which suggests the need for new ways to prevent the formation of cavitary lesions and cysts in patients of TSCI. [2] Previous work suggests that treating secondary injury is critical, and that chronic neuroinflammation can be managed by minocycline therapy, though intrathecal penetration from systemic delivery is problematically low. [8]

Intervention Background

Minocycline

Minocycline is the only drug that treats the secondary injury in SCI, and does so by addressing most of the major causes. [10] It is a tetracycline antibiotic that has currently not fully understood anti-inflammatory behavior. It exhibits neuroprotection after SCI, improves functional recovery, and reduces progressive tissue loss, through it anti-inflammatory, anti-oxidative, and anti-apoptotic properties. [5-7, 10]

In mice, it has been shown to reduce tissue damage and extent of loss and improve the return of strength and function of the impaired bodily regions with histological studies showing preservation of nerve tracts that correlated with higher behavioral scores on the Basso Beattie Bresnahan locomotor scale. This improvement was observed as early as 3 days after injury when compared to a control group, and the improvement continued while the untreated mice reached a plateau in their recovery. Even more clinically important, the minocycline treatment group outperformed a test group receiving the current leading conservative therapy, methyl prednisone. [5]

Minocycline has been evaluated for treatment of noninfectious inflammatory disease in humans, such as treatment resistant rheumatoid arthritis. It has a high penetration throughout the body, outside of the central nervous system, and even when used predominantly as an antibiotic it was suspected to have utility in treatment of cystic fibrosis. Relevant observations were attributed to an effect of minocycline that is unique within its drug class: inhibition of leukocyte migration. [6] Minocycline reduces tissue loss, with better outcomes than the current best conservative therapy, methyl prednisone. [10]

Currently the mechanism of minocycline neurological anti-inflammation has numerous approaches. It inhibits microglial activation, obstructs the mitochondrial calcium overload that triggers apoptosis and upregulates anti-apoptotic factors, and minocycline controls reactive oxides and the effect of free radicals. [7, 10]

In humans, 1-5 days of treatment has been shown to be sufficient for neuroprotection in SCI and reduce secondary injury at local doses of 35-75 µg/mL. A recent Phase II clinical trial tested doses of 12-22.5 mg/kg/day (the standard human dose is 3 mg/kg/day), and observed poor intrathecal penetration with a local dose of only 2.3 µg/mL. This trial also uncovered signs of hepatocellular toxicity in a patient at this dosage, in the form of elevated liver enzymes. [10]

The minimally effective dose for anti-inflammatory effects alone is 0.5 µg/mL, but the neuroprotective dosage is much higher, as mentioned. 1.5-50 µg/mL prevent mitochondrial cell death pathways and glutamate toxicity. 10-40 µg/mL prevent hemorrhage induced toxicity. 35-75 µg/mL prevent excitotoxicity and Ca^{2+} influx. [10]

Minocycline also suppresses release of cytokines which may disrupt the blood brain barrier. In different models, minocycline had potential to help treat the progression of the following diseases: Parkinson's Disease, Huntington's Disease, Alzheimer Dementia, Multiple Sclerosis, Amyotrophic Lateral Sclerosis, and Stroke. All of these diseases are characterized by progression, changes in cell count and myelination, and micro-infarct and inflammatory processes. Minocycline suppressed t-cell proliferation in experimental models of autoimmune encephalomyelitis. [7, 8]

Systemic treatment with minocycline in humans, at the high doses needed for central nervous system (CNS) penetration has been associated with a myriad of side

effects, even in conventional use. Most concerning, vestibular effects have been found in up to 70% of female study subjects. Other side effects include nausea, vomiting, weakness, loss of concentration, headache, visual problems, skin rashes, and tinnitus. [11]

For these reasons, a local delivery system has great therapeutic potential. One approach is to load minocycline in stable, slow release particles, and delivery a particle loaded hydrogel reservoir to the injury site, such as shown in the diagram in Figure 1.

Dextran Sulfate and Metal Cations

Therefore, there is potential in a localized, controllable drug delivery system that can give small doses of minocycline to target tissues that would allow for therapeutic treatment levels where needed, but keep systemic dosing well below that which may have adverse effects. Polysaccharides are currently viewed as a promising vehicle for nanoscale drug delivery and are becoming more widely studied as such. They can be crosslinked covalently or ionically, can form polyelectrolyte complexes from electrostatic interactions, and can form self-assembled structures due to hydrophilic and hydrophobic interactions. [8, 12]

Ionic crosslinking of polysaccharides is a fast, low cost, and efficient method of forming polysaccharide matrices for drug loading, while covalent crosslinking is more expensive, slower, and requires more extreme lab conditions to perform. [12] Different methods can be combined to further tune a drug carrier. The polysaccharide dextran sulfate is a biocompatible polymer that has been shown to have a high binding affinity for divalent metal cations, which allow it to bind to minocycline. [8] It can form ionically

crosslinked matrices in the presence of cations and minocycline, with minocycline acting as the inducer and linker. [8, 12] In Figure 2, red boxes represent metal ion chelation sites and the blue box represents the site of direct DS – MH interaction. [8]

This particle loading can provide time and dose control over drug delivery. [10]

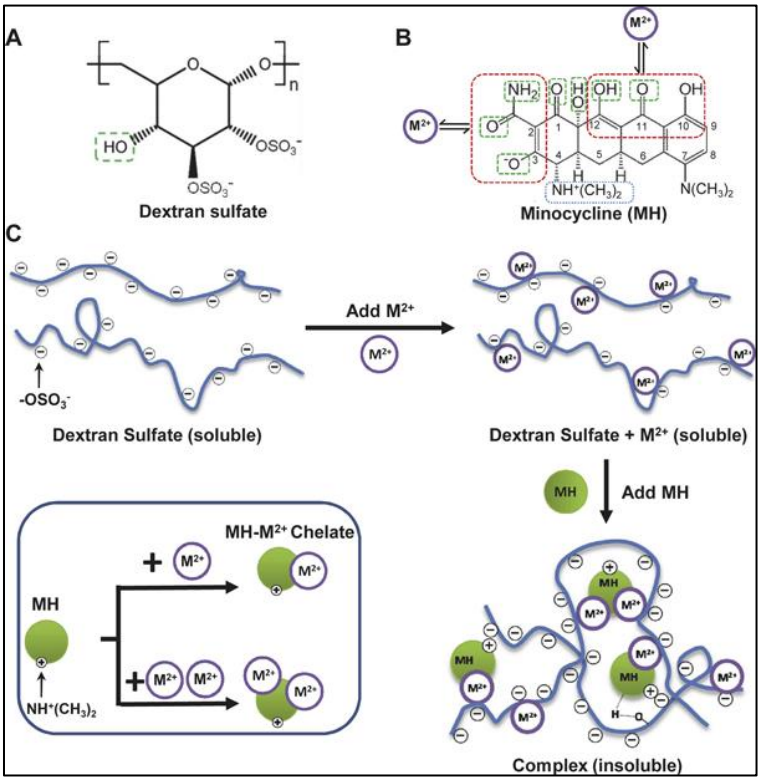

Figure 2: Schematic from previous work for particle formation

Z. Zhang, et al. "Metal ion-assisted self-assembly of complexes for controlled and sustained release of minocycline for biomedical applications," Biofabrication, vol. 7, p. 015006, 2015.

Hydrogel Loading

Local delivery requires control over localization of the drug reservoir. A biocompatible hydrogel, such as agarose, can be used to maintain the position of the particles over the injury site. In combination with particlization, hydrogel loading opens the possibility of

maintaining a local drug reservoir that can be held in place for a set duration without the drug being washed away by bodily fluids. [10]

Mechanism and Need for Model

Currently the dose that can be delivered from previously studied entrapment methods is stable and long lasting, as seen in Figure 3.

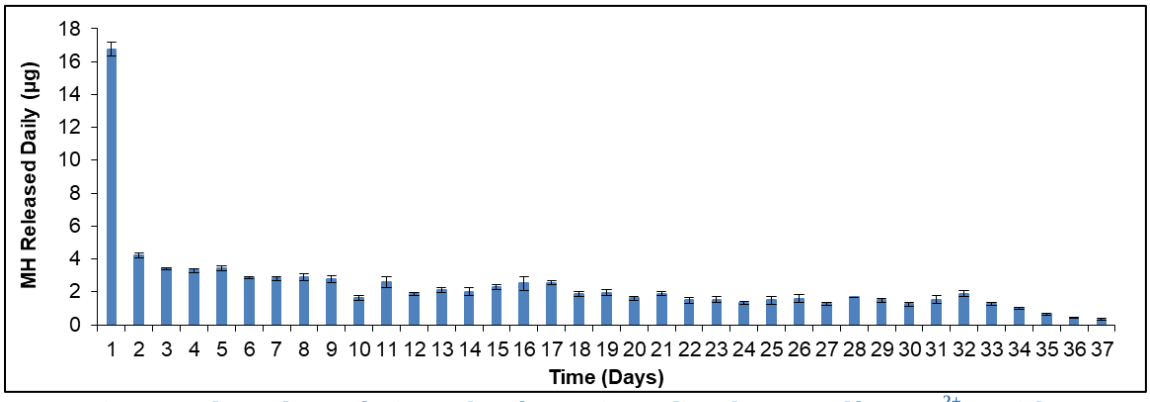

Figure 3: Slow release of minocycline from minocycline-dextran sulfate-Mg^{2+} particles

Z. Wang, et al. "Local delivery of minocycline from metal ion-assisted self-assembled complexes promotes neuroprotection and functional recovery after spinal cord injury", Biomaterials, vol. 112, pp. 62-71, 2017.

The combination of minocycline hydrochloride (MH), dextran sulfate (DS), and a divalent metal cation, such as magnesium, forms a self-assembling, water insoluble complex with a proposed chemical reaction of:

$$(1)\ MH + DS + Mg^{2+} \xleftrightarrow{k_{for}/k_{rev}} [MH - DS - Mg^{2+}]$$

This particle formation has very high drug entrapment with a slow and stable release of minocycline. The system overall is pH dependent, as the ionic interactions change with

pH, which offers a degree of control for innate dosing changes relative to local inflammatory acidosis. [8]

Bioactivity analyses and neuroprotection studies have showed efficacy of released MH. The anti-inflammatory minimal effective local dose of 0.5 μg/mL was not high enough for neuroprotection, but further studies aim to better control this release. [8]

Current understanding of this mechanism requires further evaluation, but some details have been studied. It requires one charged polymer (DS), forms an insoluble complex, and requires all 3 components to form. FTIR has suggested that the sulfate and hydroxyl groups on DS react with MH, the sulfate group also can bind the cation, and there is a chelation site for cation binding on MH (C_{10}-C_{12}). MH has a potential second metal binding site. Direct interaction with DS is possible by forming a positively charged ammonium group that could directly form an ionic bond to the negative sulfate group on DS. However, no insoluble bonds form between any 2 of these components, despite evidence that suggests that any 2 will react. [8]

Therefore, a proposed mechanism suggests that crosslinking of DS is needed, and one MH molecule can bind to two DS sites through either cation bonding, electrostatic interaction, or hydrogen bonding. At least one of these bonds however must be cation bonding, as the other two are not strong enough to maintain a complex. The peak complex occurs at a DS:MH ratio of 1.2:1 by mass concentration (empirically derived, molecular weight of DS is variable), and corresponds to a molar ratio of sulfate:MH of 3:1, suggesting that higher or lower concentrations of DS to MH leave one in excess relative to the other. Increasing the cation concentration does raise MH loading by increasing DS binding, but only until some saturation concentration. [8, 10]

Thesis Statement

To better predict the behavior of this drug vehicle, and to better direct further studies, it is important to find the relationship between the parameters of vehicle creation and the resulting particle characteristics and drug release profiles. This relationship can be used to model the drug release of a given proposed vehicle composition, and therefore be used to direct research or even therapeutic development.

Design Component

Overall Problem

The overall goal for this investigation is to tailor a delivery system for local and controlled drug dosing. Patients with SCI need a sustained and stable injury site exposure to minocycline at levels that are systemically toxic, and a chelation particle formulation is capable of high levels of entrapment of minocycline with slow release. [8] The release of this system varies as the starting concentrations of its constituents are changed, but optimization of the delivery has yet to be completed and the mechanism is still unclear.

Therefore, it is intended for the work of this study to further the understanding of the system while also completing its design to deliver a therapeutic dose of minocycline for mitigation of secondary injury in SCI.

Specific Problem

As the drug release can be affected by changes in the initial conditions of all three components, there are many conditions that need to be evaluated for any release profile or effect characterization. [8] Due to the complexity and cost of experimentation, as well as the time necessary for such studies, there is a need to be able to predict the profile and therefore choose the right conditions to test for optimal vehicle characteristics.

Since the mechanism of drug entrapment and release is not yet fully described in this novel system, it is also important to better understand how the formulation relates to its function. Once again, testing every possible combination of conditions is impractical,

and there is need for a method to predict ranges of outcomes and trends of vehicle behavior for a chelation based drug delivery system.

Model Design

Evaluation of the problem and the obstacles in both optimizing a system and characterizing a mechanism has shown that there is room for predictive modeling in drug delivery investigations. Discussions with drug development labs both in academia and industry have shown that there is a broad interest in simple approaches to modeling drug release, where a lack of expertise for modeling complex systems is the large obstacle to implementation of modeling processes in current approaches, as confirmed in an interview conducted October, 2016, with Boris Polyak, PhD, Assistant Professor of Surgery at Drexel University College of Medicine.

Therefore this investigation of the biomedical engineering skill-set should combine the engineering design approach of organizing a system in fundamental sections, the scientific principles of evaluating chemical behavior, and the math and computer skills needed to render these entities in a usable form. It is intended that a model of drug release behavior can support or reject proposed mechanisms and reduce the number of conditions needed to consider for system optimization. The objective of this design is to characterize a chelation particle system as a function of controllable input parameters and then apply it to minocycline entrapped with dextran sulfate and magnesium cations.

Vehicle Design

After the generation of a model, this investigation should implement it. As stated, the overall problem is still developing and understanding a method of local drug delivery for a specific problem, and the model itself is a means to that end. The objective of this design is to present a system that can release a sustained, controlled dose of a minocycline from the chelation particle vehicle.

Aims

Specific Aim 1: Determination of the effect of controllable parameters on minocycline.

There are 3 components to this drug release vehicle within the hydrogel: the drug (MH), the polysaccharide residue (DS), and the chelator (Mg^{2+}), which at specific concentrations results in a system that has high entrapment and very stable release. Each of these components can be manipulated for their initial concentration at the Control level as well as a High and Low value.

The first aim of this study is then to determine the effect of these parameters on the release of MH through a factorial designed experiment. High entrapment efficiency occurs at binding sight saturation which is determined by the initial concentrations of components. Therefore the highest entrapment efficiency condition should represent the most stable and lowest dose release. [8, 10] There are expected to be observable trends of release behavior relating to entrapment efficiency and these effects are to be characterized. As there are ratios between the particle constituents that will result in different particle stability, and previous work has suggested the most stable form of the particle [8], this aim will investigate the behavior of drug release for different initial conditions.

Specific Aim 2: Design of a mathematical model to predict daily release of bound minocycline from a hydrogel.

The second aim of this study is to develop a mathematical model to predict the daily release of a drug from a chelation bound particle loaded within a hydrogel source. This includes both a general applicability as well as system specific functionality for the drug delivery vehicle being studied.

The complexity of this system can be evaluated as a combination of more simple problems. Execution of this aim will involve the application of scientific principles to derive mathematical representations of system behavior. This includes the formation of a usable form of the model and comparisons between model output and empirical data. Ultimately, simplification of the system's transport processes and quantification of constants in control conditions will define the drug release behavior.

Below are the steps that comprise this aim.

I. Development of model
   a. Simplify components of system and overall transports process
   b. Quantify constants, assuming the control conditions
II. Evaluation of model
   a. Verification
      i. Generate field of outputs and compare to empirical data of control conditions gathered in Aim 1
   b. Validation
      i. Compare output of model to empirical data for High and Low concentration conditions of Aim 1

Specific Aim 3: Application of a model to guide optimization of a modifiable drug delivery.

The design of a model is a means to the end of presenting a method of delivering MH at desired doses. Therefore, without application of the model, the overall purpose is not met. Therefore, the third aim is to use the model outputs to increase understanding of the mechanism of delivery and propose conditions that can yield unique, discrete, and specific drug release results specific to this system.

Design Inputs

See Table 1 for the traceability matrix from design criteria to validation. The model must have a reasonable amount of accuracy, predictive behavior, and usability.

Table 1: Traceability matrix for design inputs and outputs

Constraints	**#**	**Criteria**	**#**	**Specification**	**#**	**Verification**	**#**	**Validation**
Simplicity within student modeling ability	***1***	Predict release above minimally relevant dose ($R^2 > 0.9$; $p < 0.05$)	***1***	Model	***1.1***	Compare model outputs to training data	***2.1***	Release studies with testing data
Equipment within lab	***2***	Able to predict release profiles for parameter combinations beyond training data					***2.2***	Follow-up release studies
	3	Usable Interface					***3.1***	Usability Analysis

Model Conceptualization and Formation

The rate of particle degradation was found in a multistep method. Using chemical simulations of semi-empirical methods through MOPAC software, the system was simplified to two parts by way of binding energies: MH and the bound DS-Mg^{2+} vehicle, which reduced the chemical reaction to a 2 component reaction with the stability of the residue-chelator bond being a function of their initial concentrations:

$$(2)\ MH + [DS - Mg^{2+}] \xleftrightarrow{k_{for}/k_{rev}} [MH - DS - Mg^{2+}]$$

Based on previous work, it was proposed that the most stable condition resulted from a ratio of DS:MH concentration of 1.2:1 mg/mL, at 7.2 mM of Mg^{2+}. This 1.2:1 ratio of DS:MH concentrations represents the condition with highest entrapment efficiency. [8] As per empirical studies, DS release can be estimated to follow zero, first, or some other order of reaction. Using half-life relationships between time to equilibrium and the rate constant, rate constants can be estimated empirically, and rate constants can be used in calculations to predict particle degradation as functions of time and concentration.

Drug release is a function of time, source concentration, sink, and diffusivity of drug through medium. In a general form, resulting from manipulation of Fick's Laws of Diffusion and conservation of mass:

$$(3)\ \frac{d}{dr}(r^2 N) = 0$$

$$(4)\ N = -D \cdot \frac{dc}{dr}$$

for *N* being flux, *D* representing the diffusion coefficient of the chemical in question through the chosen medium, *r* representing the radial axis from the center point of the sphere of hydrogel, and *c* representing the molar concentration of free drug within the

hydrogel. With assumptions of pseudo-steady state, that the rate of reaction of particle formulation and degradation being on a different order than that of diffusion, there is no other reaction being considered in the movement of the drug. It can also be assumed due to the dilute drug release into the release media, that there is an infinite sink for diffusion purposes.

Applying a shell balance, where the amount of mass in a shell is constant at a specific point in time, the product of flux and surface area is constant. For a changing concentration over time but stable hydrogel volume, this can be written as:

$$(5)\ W = N \cdot SA = -\frac{V}{M} \cdot \frac{d\rho}{dt}$$

for *W* moles of drug in the shell, *SA* surface area of the shell, *V* representing volume of the hydrogel bead, *M* molar mass of the drug, *t* being time, and ρ meaning mass density of the drug. Manipulation of Equations (3) and (4) result in two equations for *W*:

$$(6)\ W = 4\pi RDc = \frac{V}{M} \cdot \frac{d\rho}{dt}$$

where R is the radius of the hydrogel bead. Boundary conditions can be assumed that at time $t = 0$, the density ρ of drug within the hydrogel is ρ_i, and at time $t = t_i$, $\rho = \rho t_f$. Integrating and solving for final density yields:

$$(7)\ \ \rho_{tf} = \rho_{ti} - \frac{4\pi RDM}{V} \cdot t_i \cdot c_i$$

The value of c can be calculated at a given moment as a function of the current concentration of the particle constituents. Given Equation (2) above, the change in concentration of MH at any point in time can be found by:

$$(8)\ \frac{d[MH]}{dt}|_{ti} = k_{rev}([MH - DS - Mg^{2+}]_0 - \Sigma[MH]_{ti-1}) - k_{for}[MH]_{ti-1}([MH - DS - Mg^{2+}]_0 - \Sigma[DS]_{ti-1})$$

This is the rate of generation of MH from degrading particles, given the changing concentrations of MH and DS. DS efflux can be more accurately estimated as a function of time based on the order of its kinetics, derived empirically. The concentration can be calculated at each time point iteratively starting from known initial conditions and entrapment efficiencies. A series of functions representing the various portions of this formula can then be used to characterize the movement of MH from the particles to the release media, with the mathematical representation of the full formula being:

$$(9)\ \rho_{ti} = \rho_{ti-1} - \frac{4\pi RDM}{V} \cdot t_i \cdot \{c[MH]_i + k_{rev}(c[MH - DS - Mg^{2+}]_{ti-1} - c[MH]_{ti-1}) - k_{for}c[MH]_{ti-1}(c[MH - DS - Mg^{2+}]_{ti-1} - c[DS]_{ti-1})\}$$

Note that the bracketed molecules denoted by 'c' are in molar concentration, representing the state within the hydrogel. This equation can be separated into components by distributing constants and separating the function that represents the generation of MH to better represent the movement of MH between the particle, free hydrogel, and media compartments. Assuming that the amount of time between ρ_{ti} and ρ_{ti-1} or the duration of t_i is 1 second, then the value for t_i at each iteration is 1, and the formula can be run iteratively to characterize MH movement over time.

Methods

See Appendix for Equipment, Software, and Materials

Gel Formulation

Particles were made *in situ* to ensure even distribution within the hydrogel. Solutions for 1.5% agarose hydrogels were prepared with final concentrations as per Table 2, using a mixture of double concentration MH in one solution, and double concentration of DS and Mg^{2+} prepared in 3% agarose (stored at 80 °C) in another, using deionized water as the solvent. These solutions were combined 1:1 resulting in the desired concentrations for all, then pipetted in 20 µL gel volumes, each condition prepared in triplicate.

All samples were loaded into a 96 well plate for release studies. Samples were maintained at 37 °C in 100 µL of release media, Hanks Buffered Saline Solution (HBSS), which is prepared according to lab protocol to mimic the intrathecal environment (formulation is listed in the appendix). Release media was replaced each day at the same time for 5 days and the concentrations of MH were measured.

Table 2: Initial conditions for drug particle loaded hydrogels

Condition	Minocycline (mg/mL)	Dextran sulfate (mg/mL)	Magnesium (mM)
Control	1.0	1.2	7.2
Low	0.5	0.6	1.8
High	2.0	2.4	14.4

Entrapment Efficiency

Using the same fabrication approach as the gel preparation, without the agarose, particles were made for the concentration conditions of Table 2. Samples were centrifuged at 10,000 RPM for 10 minutes to separate particles from solution. Release for MH was taken from each supernatant and the ratio of free MH to total loaded MH was recorded. This was done both as part of the investigation for Aim 1, as well as to provide initial values of free MH within the hydrogel depending on the conditions used to prepare them.

Release Studies: Minocycline

At the same time each day for 5 days, MH was measured at 380 nm light using the *NanoQuant* spectrometer, for 40 µL of media. Absorbances were converted to release media drug concentration and released drug mass by a standard curve generated from the stock solution.

Model Generation

After simplifying the system to components, constants were empirically derived. Diffusion of MH from the agarose hydrogel was evaluated by loading 20 µL 1.5% agarose hydrogels with 1 mg/mL MH and measuring drug release at 5-10 minute intervals. Manipulations of Fick's law and shell balance, Equations (5) & (6), were used to calculate the diffusion coefficient.

$$(10)\ D = \frac{V}{4\pi R}\frac{d\rho}{dt}$$

The half-life of reaction equilibrium was evaluated by forming particles at the control concentrations without agarose. Samples were made for time points of 5-10 minute intervals. At its time point, each sample was centrifuged at 10,000 RPM for 10 minutes to remove particles, and the MH concentration of the supernatant was evaluated. Assuming first order kinetics, the rate constant of particle degradation (k_{rev}) was estimated using the half-life of particle degradation. The rate of particle formation (k_{for}) was also estimated based on the rapid formation of particles.

As per empirical data (see Results), DS release follows a half-life time pattern that is fairly constant regardless of concentration or time that suggests a first order kinetic reaction for particle degradation which has a half-life relationship of:

$$(11)\ t_{1/2} = \frac{ln(2)}{k_{rev}}$$

The system equilibriates more rapidly than the used measurement methods, while diffusion of free drug can be captured by daily release, therefore these occur at rates that differ enough to suggest a pseudo-steady state system for drug release to diffuse media with regards to free drug generation. [13] At equilibrium, the equilibrium constant can be found, from which the rate constant in the opposite direction can be derived:

$$(12)\ K_{eq} = \frac{[MH]\cdot[DS-Mg^{2+}]}{[MH-DS-Mg^{2+}]}$$

$$(13)\ K_{eq} = \frac{k_{for}}{k_{rev}}$$

Using the principles discussed in Model Conceptualization and Formulation section, the mathematical model was then derived with these constants.

Model Verification and Validation

The model was written into *MATLAB* as a function and then used to predict the daily release of the control condition over 5 days. This was compared to the empirical results with the *corrcoef* function, which provides the correlation of coefficients (R^2) as well as a measure of statistical significance. For validation, to see if the model was applicable when the particle stability was altered by changing the initial conditions, the outputs for High and Low concentration conditions were then compared to empirical data as well using the same method of comparison.

The *corrcoef* function provides correlation and significance analysis for nonlinear and noncategorical data, as opposed to a Pearson's Goodness of Fit, while representing trend accuracy as opposed to error sum methods. The conventional *p* value of $p < 0.05$ was used as the threshold of significance.

System Optimization

With the presumed successful verification and validation of the model complete, analysis of the behavior of the vehicle was to be assessed using statistical comparisons to test for significantly different release profiles. Empirical data was used when model data was not sufficient. In the event of a lack of significant differences in release profiles, or with a poor correlation, optimization would be beyond the scope of this study. Otherwise, optimized system parameters would be chosen by model outputs as choosing the initial conditions that resulted in the most favorable release profile.

Model Usability Analysis

The final *MATLAB* function was then evaluated to test for its usability. Qualitative goals were to ensure a limited number of inputs and steps to generate output data.

Results

Empirical Data from Release Studies

In Table 3 the release results from experimentation are presented for MH. It can be observed that the control condition has the lowest mass release of MH over time, and remains largely stable, despite an aggressive burst dose. High Mg^{2+} and high MH initial loading present with larger bursts, and all samples trend towards similar profiles as control after the first day. ANOVA of the release shows that the different conditions do have significant differences ($p < 0.001$). Not including the highly variable Day 1 release, the different conditions still did have statistically significantly different outputs, even if there is overlap of their values and a trend towards control condition behavior ($p = 0.0016$).

Table 3: Daily release of minocycline from particle loaded hydrogels

Day	Control	Low Mg2+	High Mg2+	Low MH	High MH	High DS
1	3.66	2.03	4.56	2.71	4.77	3.56
2	1.00	0.89	1.26	0.86	1.22	1.10
3	0.96	0.88	1.00	0.86	1.08	0.91
4	0.83	0.80	0.80	0.75	0.94	0.89
5	0.75	0.77	0.79	0.73	0.90	0.83

Daily releases can be more easily observed in Figure 4 below, which summarizes the table.

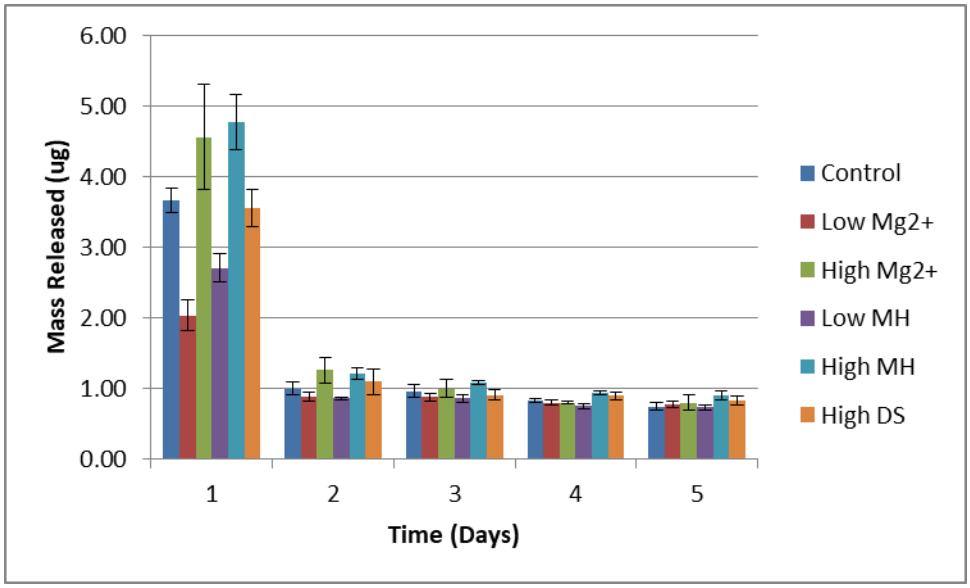

Figure 4: Daily observed mass release of minocycline

Entrapment of MH varied by initial conditions and the entrapment efficiencies for each are shown in Figure 5.

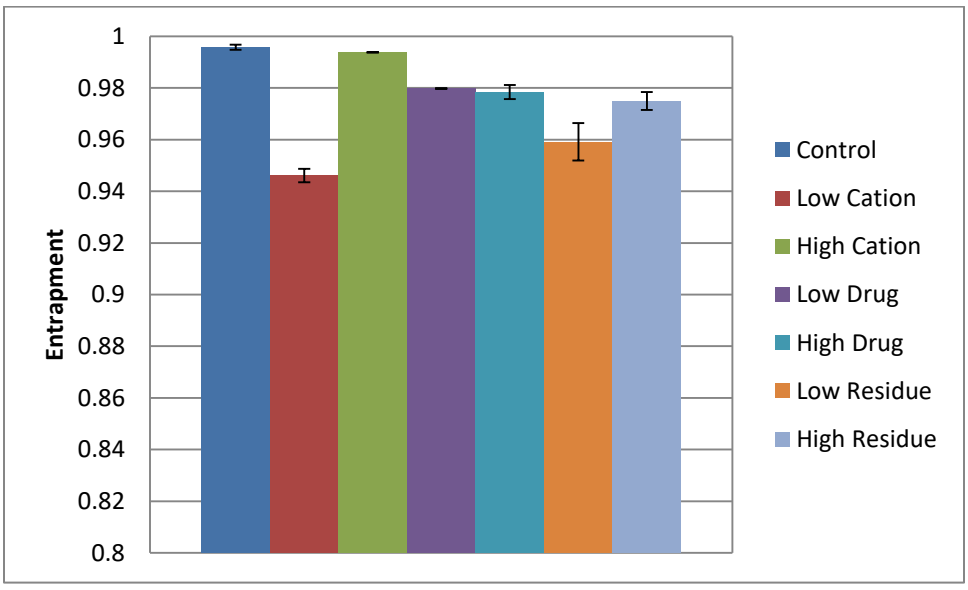

Figure 5: Minocycline entrapment by condition

As per semi-empirical simulation for mechanical binding via MOPAC, the mechanical binding energies of the different component combinations are -4,791 eV for DS-Mg^{2+}, -5,494 eV for MH-Mg^{2+}, and -10,619 eV for all 3 combined. MH alone is -5,814 eV while DS alone is -4,771 eV. This reveals an energy of binding for MH to DS-Mg2+ of -15 eV and DS to MH-Mg^{2+} of -354 eV which is less stable. This suggests that DS complexes with Mg^{2+} with significantly more stability than MH does, allowing for the treatment of DS and Mg^{2+} to be treated as a subunit for model simplification purposes, assuming constant energy of binding.

Diffusion Coefficient Estimation

Figure 6 shows the plot of the diffusion coefficient (D) in m^2/s empirically derived by point measurements in time (min). The value plateaus near $2x10^{-12}$ m^2/s after the values for D stabilize and plateau.

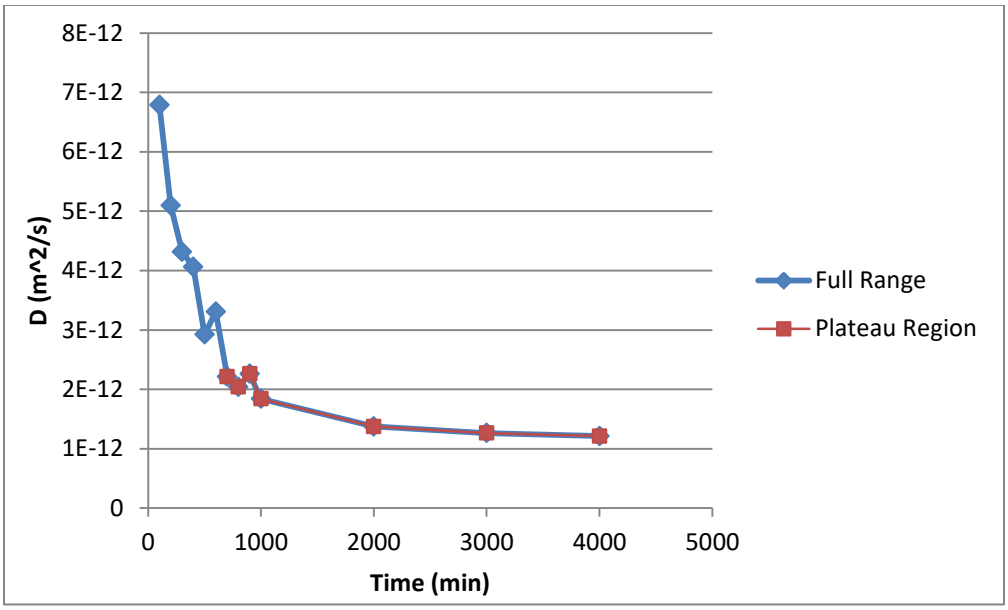

Figure 6: Diffusion coefficient of minocycline in 1.5% agarose

Rate Constant Estimation

As shown below in Figure 7, the system reached equilibrium fairly rapidly that showed negligible change over time, and the relative concentrations yielded an equilibrium rate constant (K_{eq}) of 0.0026 1/s, using an average of the results for time before the initial time point. As a result, with a small magnitude of time assumed for the half-life, the particle degradation rate constant (k_{rev}) was found to be 0.0145 1/s using a similar estimation of time until the midpoint between fabrication and the first time point. Using the relationship between these rate constants, the particle formation rate constant (k_{for}) was found as 0.000038 1/s, many orders of magnitude smaller than the degradation rate constant.

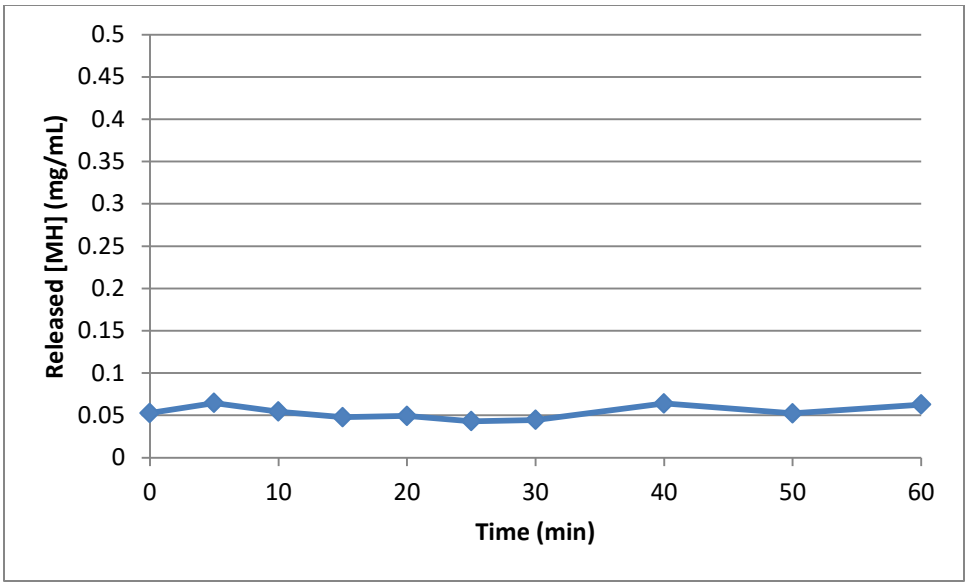

Figure 7: Equilibrium state: concentration of released supernatant

Entrapment Efficiencies

The entrapment efficiencies of MH for each tested condition were used to create an entrapment map as a function of all three variable initial conditions. As the lowest entrapment was still well above 90%, it was assumed that the loss of efficiency was not additive and for simplicity was treated as a series of linear relationships. Between the low and control conditions and control and high conditions, individual lines were generated, as seen in Table 4. If multiple conditions were varied, these entrapment efficiencies were averaged rather than compounded. Entrapment Efficiencies were calculated as a line function of chosen concentrations of MH and DS in mg/mL, and Mg^{2+} in mM.

Table 4: Coefficients of line between tested points for entrapment efficiency

Condition	Low Mg2+ : Control	High Mg2+ : Control	Low MH : Control	High MH : Control	Low DS : Control	High DS : Control
Line Slope	0.009	-0.00027	0.001	-0.017	0.061	-0.017
Line Intercept	0.930	0.998	0.979	1.013	0.923	1.017

These lines comprise an entrapment efficiency map that can used to interpolate the initial concentration of bound and free drug within the hydrogel upon particle formation. See Figure 8 for map.

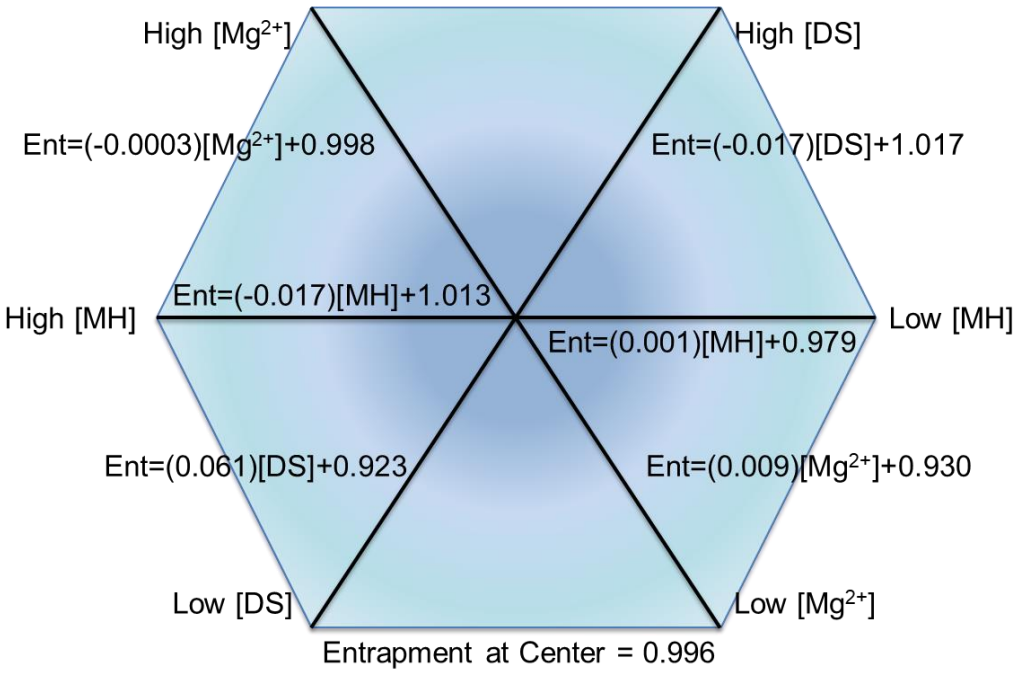

Figure 8: Entrapment Efficiency Map

This assumption was challenged, by testing entrapment efficiencies at the midpoints of each line, and then 3 random combinations of variable manipulation. The results are shown in Table 5. It can be observed that the assumption does not actually hold

consistently so there is some more complexity to the entrapment mechanics. The concentrations used for the components are listed in the table, and the same method was applied for particle formation and testing as before.

Table 5: Entrapment efficiency linearity assumption challenged

mM Mg	**4.5**	**10.8**	**7.2**	**7.2**	**7.2**	**7.2**	**4.5**	**10.8**	**4.5**
mg/mL MH	**1**	**1**	**0.75**	**1.5**	**1**	**1**	**1.5**	**0.75**	**0.75**
mg/mL DS	**1.2**	**1.2**	**1.2**	**1.2**	**0.9**	**1.8**	**0.6**	**1.2**	**1.8**
Predicted Value	0.971	0.995	0.980	0.988	0.978	0.986	0.973	0.990	0.979
Average Measured Value	0.911	0.967	0.748	0.912	0.910	0.980	0.566	0.700	0.201
Standard Deviation	0.009	0.004	0.005	0.038	0.012	0.002	0.057	0.093	0.043
Percent Error	0.06	0.03	0.24	0.08	0.07	0.01	0.42	0.29	0.79

Model Usable Form and Output

The final form used for application was the matrix formula of the final equation above, Equation (9). After conversion of mass density to molar concentration, the system takes the form of Equation 14 below:

(14)

$$\begin{Bmatrix} c[MH]_{ti} \\ c[MH-DS-Mg^{2+}]_{ti} \end{Bmatrix} = \begin{Bmatrix} 1-\frac{4\pi RDM2}{V}t_i & -k_{rev}\frac{4\pi RDM2}{V}t_i \\ -\frac{4\pi RDM2}{V}t_i & 1-k_{rev}\frac{4\pi RDM2}{V}t_i \end{Bmatrix} \begin{Bmatrix} c[MH]_{t0} \\ c[MH-DS-Mg^{2+}]_{t0} \end{Bmatrix}$$

Output of the predicted daily mass release of MH is shown below in Table 6. This table and Figure 9 below provide the output data for the same test conditions empirically evaluated, as generated by the model derived in this experiment. The subsequent figures (Figure 10 - Figure 15) provide graphical comparisons of data output by individual condition to empirical data. Different conditions did have different modeled release profiles, as per ANOVA analysis ($p = 0.049$). It can be observed that the model captures a genuine profile only in some of the cases, though aggressively moves towards a daily release of zero in more conditions and without observable pattern, and therefore cannot be said to accurately portray daily release.

Table 6: Model output of minocycline daily release by mass (µg)

Day	Control	Low Mg2+	High Mg2+	Low MH	High MH	High DS
1	0.06	4.13	0.21	0.70	2.90	1.68
2	0.00	2.30	0.00	0.23	0.99	0.65
3	0.00	1.63	0.00	0.06	0.29	0.27
4	0.00	1.08	0.00	0.00	0.00	0.00
5	0.00	0.64	0.00	0.00	0.00	0.00

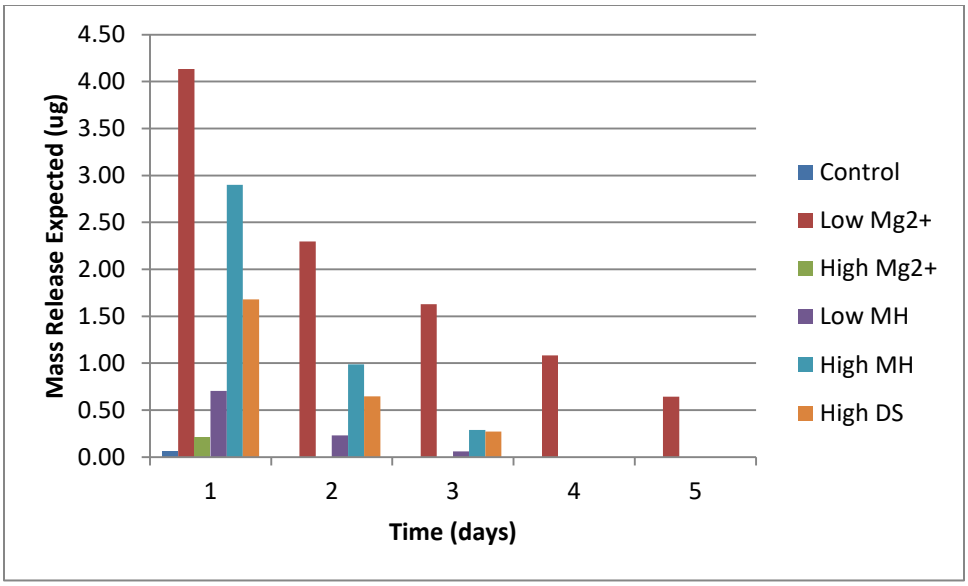

Figure 9: Daily predicted mass release of minocycline

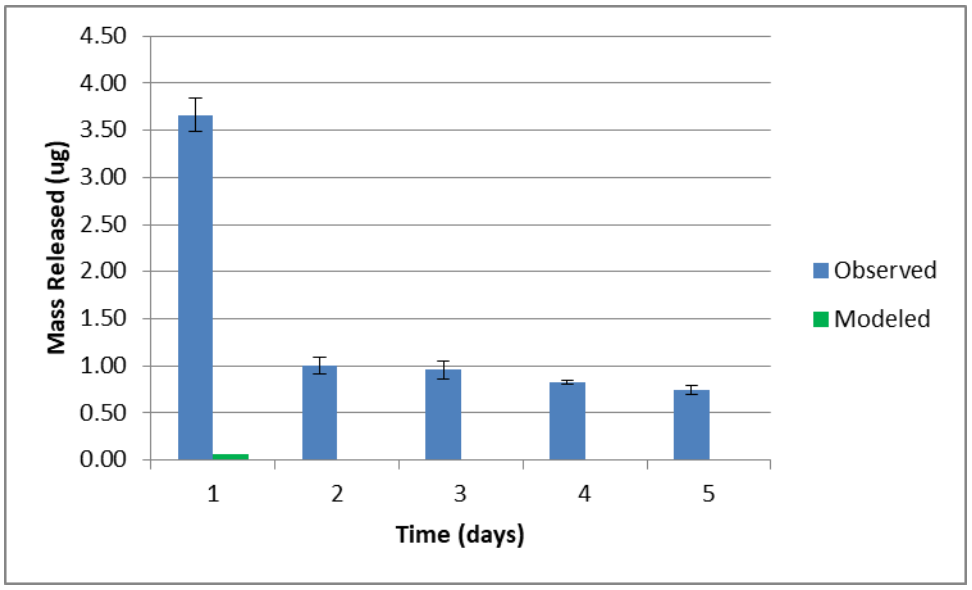

Figure 10: Modeled and empirical data for Control condition

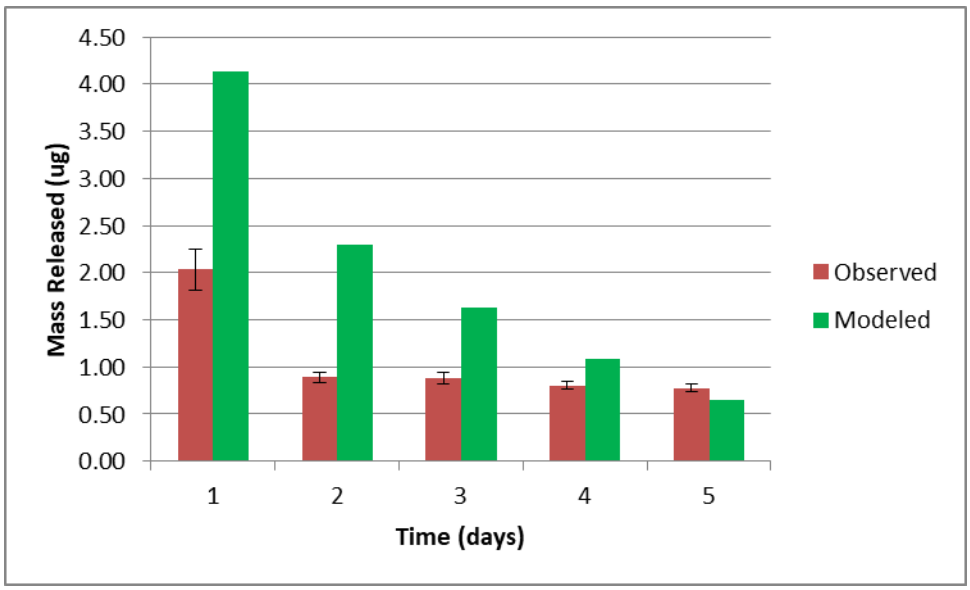

Figure 11: Modeled and empirical data for Low Mg^{2+} condition

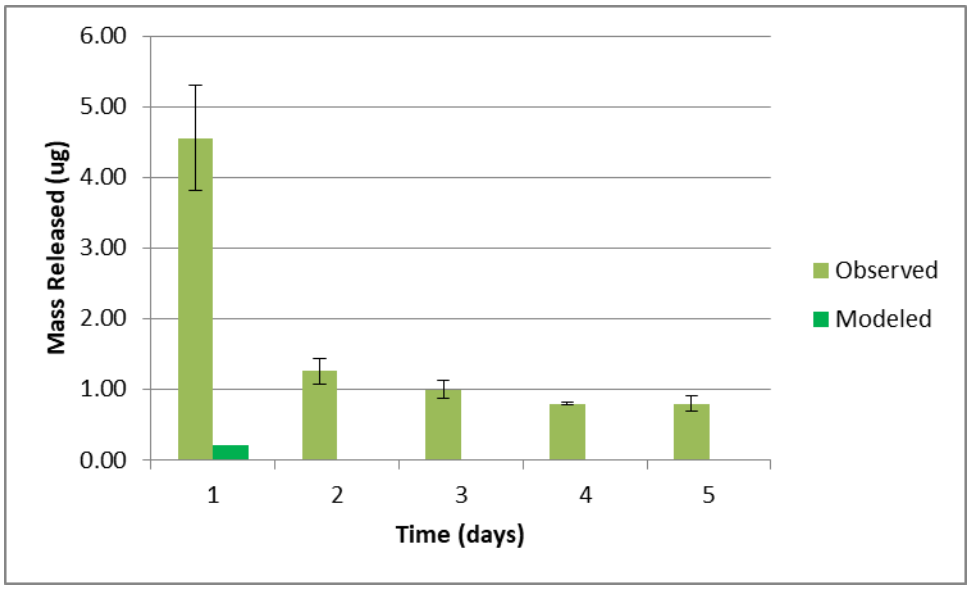

Figure 12: Modeled and empirical data for Low Mg^{2+} condition

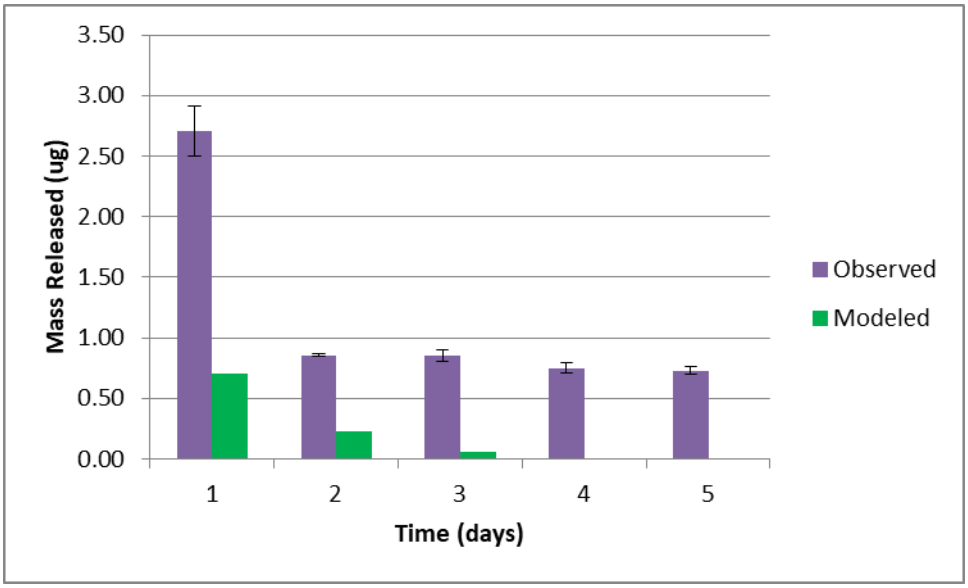

Figure 13: Modeled and empirical data for Low MH condition

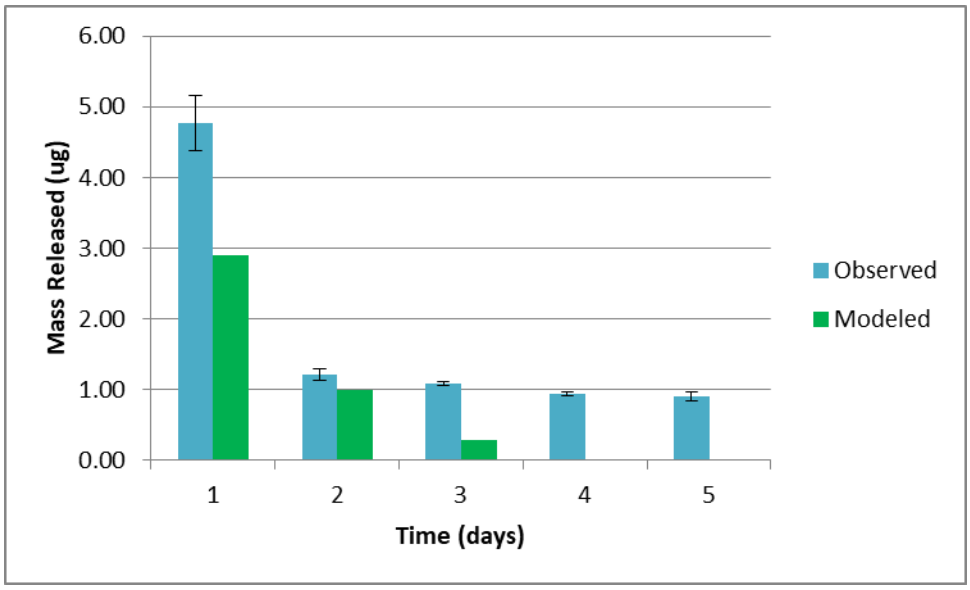

Figure 14: Modeled and empirical data for High MH condition

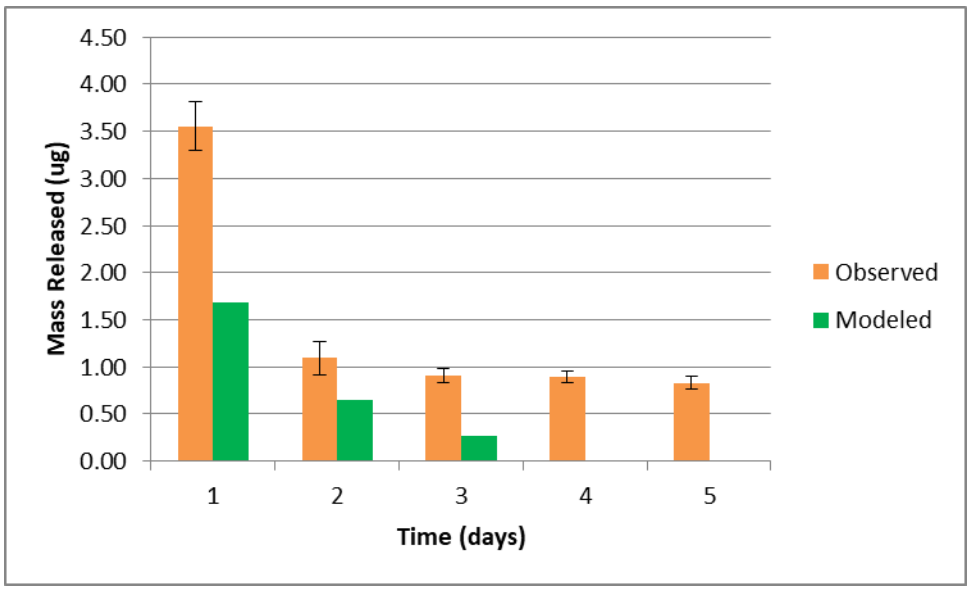

Figure 15: Modeled and empirical data for High DS condition

Model Verification and Validation

Because the data was not categorical, a correlation of coefficients rather than a Pearson's Goodness of Fit Test was used to assess the error between the expected and empirical data, with a target of $R^2 = 0.9$. The reported R^2 value was much lower, at 0.39. However, statistically, significance was also evaluated and despite the low correlation of coefficients, there was statistical significance in the model's output ($p = 0.033$). This verifies that the model statistically projects trending behavior, but not with applicable accuracy.

The model's performance for low concentrations was poor, rapidly reaching no release despite the presence of clinically relevant doses. As a result, its outputs did not validate the model successfully. Individual correlations are high with statistical significance, but this is likely due to the trend being in the right direction of stable to declining dose amounts, even if the accuracy is poor.

	R^2	*p*
Overall	0.39	0.0033
Control	1.00	0.0002
Low [Mg^{2+}]	0.93	0.0241
High [Mg^{2+}]	0.99	0.0007
Low [MH]	0.96	0.0087
High [MH]	0.96	0.0079
High [DS]	0.95	0.0124

Figure 16: Summary of verification and validation results

Model Usability Analysis

A summary of usability is as follows. Inputs were simplified to the concentrations of initial particle components using the conventional units for the rest of this experiment. Because the volume of the gels and release media were held constant, they were not used as variables. Entrapment efficiency was automatically calculated for the series of entered concentrations to generate starting conditions for simulation. The output was a matrix summary of daily release concentrations by mass in µg, and a graphical representation of the same for rapid analysis. Figure 17 below is a sample output graph that was generated for the empirical conditions.

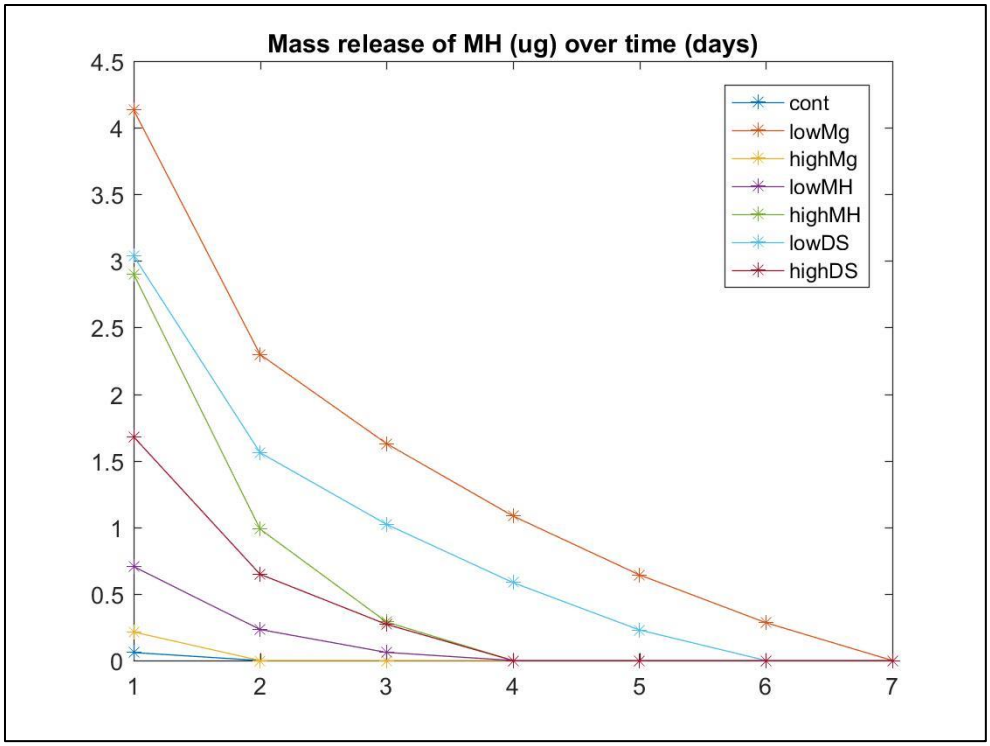

Figure 17: Sample output of daily release profiles of the empirically evaluated initial conditions

Potential for Optimization of System By Manipulation of Concentrations

Looking at the system being studied, in order to effect control by manipulation of starting concentrations of particle components, the significance of the differences in drug release was tested. Results of ANOVA stated that there was a significant difference between the different release data sets ($p < 0.001$). However, without including the burst release from day 1, the system still has significant variability between conditions ($p = 0.0016$). There is potential for optimization, though not without a more accurate model.

Discussion

Summary of Aims

Aim 1: Determination of the Effect of Controllable Parameters on Minocycline. – Aim Met

Conditions were chosen to bound the problem using high and low concentrations surrounding a high entrapment configuration for particle fabrication. Release of replicates performed as expected with the control having a low initial burst and a stable, fairly uniform long term release. The varied conditions each had lower entrapment and less particle stability as the saturation of binding of constituents was less complete when outside of optimal ratios. [8, 10] This was consistent with previous work and proposed behavior of the system.

The most stable release occurred in the conditions with the highest entrapment efficiency. Excess of components resulted in still stable conditions, as extra-saturation concentrations were lost over time. Shortage of components relative to control resulted in less MH loading but still strongly bound MH; this would present with a faster initial release that trended toward control.

This suggests that behavior is a function of both MH release from particles as well as the entrapment efficiency that determines the initial amount of free MH. The system does have saturation points, which was confirmed by the burst release initially of the high MH loading condition, that lead to a profile similar to that of the control condition.

After Day 1 release, the differences between the conditions' daily release values were blunted. There was low variability in results, consistency with previous results, and the release did start faster for less stable particle conditions, as predicted. High

entrapment conditions had low daily release, and high MH loading was rapidly depleted until control behavior was approached.

While the statistical significance of the differences between the conditions after Day 1 did not suggest a high potential for dosing modifications, distinct release profiles were made of MH as a result of this experiment and related to entrapment.

Aim 2: Application of a Model to Guide Optimization of a Modifiable Drug Delivery. – Aim Partially Met

The proposed model design presents release data as a function of the aforementioned traits of the system. Incorporating empirically derived constants for diffusion and particle degradation reaction rate provided specificity to this system to an otherwise abstract model. This model represents the various strengths of the field of biomedical engineering scientific and other principles: fundamental sciences (chemistry and physical transports), mathematics (linear algebra and differential equations), programming (*MATLAB*), lab techniques (empirical data collection), experimental design (derivation of constants), and collaboration (with topic experts in programming, mathematics, and chemistry).

As the entrapment efficiency was shown to be a function of the initial loading conditions, the derived model applies these principles and concepts to the initial conditions of particle formation. Furthermore, as the general form of the model was found without calculating specific values as determined by this specific system, it is theoretically translatable to any chelation based drug delivery system.

However, statistical testing showed that the accuracy of the model lacks the fine number and low concentration fidelity necessary for a system that changes with such small margins. While it statistically showed trend behavior of the system overall, it did not yield accurate results for specific condition predictions and the correlation of model output to empirical data was too poor for practical application for most conditions.

Therefore, Aim 3 was partially met by the specific design component of this thesis.

Aim 3: Application of a Model to Guide Optimization of a Modifiable Drug Delivery. – Aim Not Met

Optimization of the drug release system overall was unable to be performed with the guidance of the prepared model. However, tuning is still possible, at the expense of more time, resources, and manpower, to empirically test all relevant conditions. This aim was to then tune the model to give distinctly different release profiles by manipulating the fabrication concentrations. In order to explore whether or not this was possible, it was first important to establish whether or not there were quantitatively distinctly different release profiles.

ANOVA of the release profiles showed that there was a statistically significant difference between the release profiles generated by broad variation of the initial concentrations. However, the overall correlation with the model was poor, despite a significant result. As a result, it was determined that with the method of manipulation being explored within this system did not allow for distinctly different enough release

profiles that could be characterized by this modeling approach. As a result, Aim 3 was not met within the scope of this study.

Limitations and Potential Next Steps

Assumptions in Model Development

For development of this model, some assumptions were made out of theoretical convention to allow for solving of the mathematical representation. Pseudo-steady state was assumed, as the rates of particle degradation and drug diffusion were dramatically different. The release media was larger than the hydrogel and the release concentrations were low enough that an assumption of infinite sink was reasonable. The hydrogel was presumed stable, therefore the diffusion coefficient would not be time dependent. The particle kinetics was assumed to be first order after qualitative assessment of drug and residue release.

These assumptions followed convention in the solution of transports related problems. However, in implementing the model, some further assumptions were made to simplify the complex formula.

Challenging Assumptions in Model Application

Those further assumptions in implementing the model can be addressed as sources of weakness in accuracy.

First, due to the differences in magnitude between the rate reactions, it was assumed that the particle formation direction could be neglected. However, the value of k_{for} was not directly determined. Because the reaction rates could not be determined with

the accuracy needed for time periods as short as that of rapid formation and equilibration of particle bound and free MH, the rate constants were based on estimations of elapsed time rather than exact time. Accuracy would be improved by more finely determined rate constants.

Second, it was assumed that DS release did not dramatically change the kinetics of the system. This was not tested further as shifting DS concentrations relative to Mg^{2+} would have resulted in different binding energies, which would have required model complexity beyond the scope of this study. However, further accuracy could have been achieved by a more robust analysis of the effects of DS release on system behavior.

Third, reactions were assumed to be first order based on qualitative analysis of release as a representation of the degradation of particles. This was not conclusively tested, and if the order of the reaction was different, reaction rate constants would have changed. As this system is not time-resolved by the methods available (particle formation occurs near instantaneously), verification of the rate order was not within the scope of this study.

Fourth, the entrapment efficiency was assumed to be a linear relationship between the bounds tested, and the combination of changing variables was assumed to be an average. The actual complexities of the specific effects of shifting concentrations on entrapment efficiency was not evaluated. Furthermore, the assumption applied throughout the release; as release changed, it is possible that the stability of the particles changed along with the reduced saturation of binding sites. This assumption was challenged and shown to be an oversimplification. Potentially a four dimensional surface map could be crafted from empirical methods and extensive sampling, from which

entrapment efficiencies could be drawn as the starting point of modeling. However this complexity was beyond the scope of the methods in this study.

Fifth, it was assumed that DS and Mg^{2+} acted in unison, as the simulated binding strength if this subunit pairing was the strongest. The concentration of Mg^{2+} was never measured during the release process, and movement of the chelator within the system remained uncharacterized due to the complexity of the measuring process and time constraints. Further accuracy would have been likely achieved had all three components been treated with the same degree of rigor as MH, though this was beyond the scope of the current study. While DS release concentrations were measured, Mg^{2+} measurements were not included in the methods.

Future Work in System Optimization

As modification of initial conditions of particle fabrication in this study was limited to changing the concentrations of the components, it is not enough to conclusively say that there is no more control available on this system. It was determined in previous work that this chelation and the binding between the units have pH dependency, as the release of MH changes; the binding strength between MH and Mg^{2+} is pH sensitive and decreases in acidic conditions. [8] This has been considered as a potential control for a smart release system, but was deemed too complex for the scope of this study.

Furthermore, a larger study with more power could be used to calculate effect sizes, which could have greater significance in system manipulation guidance than correlation.

Final Analysis and Closing Remarks

Design Component

While Aim 2 was only partially met, it is important to note that the designed model did have statistical significance in its weaker correlation with the trending behavior of the system. While there is clear room for improvement, it cannot be disputed that there is utility in a simple approach to modeling when characterizing a drug delivery system. Using the fundamental skill set of a biomedical engineer in conjunction with general engineering design approaches, a formula was developed that characterizes the overall behavior of a complex system.

Furthermore, this model supports the current understanding of the system, from a theoretical perspective. It represents, if crudely, the empirically supported position that particle formation and drug entrapment are dependent on the initial conditions of fabrication, and the entrapment efficiency does set the tone for subsequent release. Higher entrapment efficiency correlates with the conditions that match suspected saturation conditions of binding, and thus also present with the most stable drug release.

Aim 3 was also not met, but this was due to the control methods within the scope of this study being exhausted, and a lack of fine accuracy within the model. Future work would be needed to further optimize this delivery system, which shows clear promise for localized delivery of MH.

Applications

One of the primary strengths of the approach used in this modeling process was the abstract form. At no point during the generation of the general form were specifics of a

MH-DS-Mg^{2+} system used without first characterizing a nonspecific state and then applying the unique parameters of the system to it. Therefore, while chelating drug systems are not common, there is obvious potential in their development, and the general form of this model, with some advancement, would be equally applicable with only minimal empirical input.

A second strength of this approach and therefore potential for application, is less specific to the general form and more a product of the development process. This was a complex system beyond the expertise of a single specialist that was modeled by breaking the different influences down to basic parts and using a minimal collaborative effort where needed. Such an approach provides affirmation of theoretical mechanisms, improved understanding of system behavior, and repeatability of results once the model has the necessary robustness. This was achieved by an understanding of what the influences on system behavior were, and by appropriately assuming where they could be treated as distinctly independent or where they interfaced with one another. While the form of the system may change, the approach itself has utility in the general effort of modeling a drug delivery vehicle.

Conclusion

Characterization of this system by use of a design process to generate a model stands as validation of the skill set of a biomedical engineer. The system does have potential for the chosen application, though the control mechanisms that would be necessary for this would likely go beyond altering the ratios of fabrication components. However, this

experiment shows the behavior trend of a system that is biologically safe and potentially an effective approach for future treatment of SCI.

References

Literature

[1] M. Devivo, "Epidemiology of traumatic spinal cord injury: trends and future implications," *Spinal cord,* vol. 50, pp. 365-372, 2012.

[2] A. Biyani and W. El Masry, "Post-traumatic syringomyelia: a review of the literature," *Spinal Cord,* vol. 32, pp. 723-731, 1994.

[3] G. Guizar-Sahagun, I. Grijalva, I. Madrazo, R. Franco-Bourland, H. Salgado, A. Ibarra*, et al.*, "Development of post-traumatic cysts in the spinal cord of rats subjected to severe spinal cord contusion," *Surgical neurology,* vol. 41, pp. 241-249, 1994.

[4] C. A. Oyinbo, "Secondary injury mechanisms in traumatic spinal cord injury: a nugget of this multiply cascade," *Acta Neurobiol Exp (Wars),* vol. 71, pp. 281-299, 2011.

[5] J. E. Wells, R. J. Hurlbert, M. G. Fehlings, and V. W. Yong, "Neuroprotection by minocycline facilitates significant recovery from spinal cord injury in mice," *Brain,* vol. 126, pp. 1628-1637, 2003.

[6] C. D. Freeman, C. H. Nightingale, and R. Quintiliani, "Minocycline: old and new therapeutic uses," *International journal of antimicrobial agents,* vol. 4, pp. 325-335, 1994.

[7] J. M. Plane, Y. Shen, D. E. Pleasure, and W. Deng, "Prospects for minocycline neuroprotection," *Archives of neurology,* vol. 67, pp. 1442-1448, 2010.

[8] Z. Zhang, Z. Wang, J. Nong, C. A. Nix, H.-F. Ji, and Y. Zhong, "Metal ion-assisted self-assembly of complexes for controlled and sustained release of minocycline for biomedical applications," *Biofabrication,* vol. 7, p. 015006, 2015.

[9] R. E. Burney, R. F. Maio, F. Maynard, and R. Karunas, "Incidence, characteristics, and outcome of spinal cord injury at trauma centers in north america," *Archives of Surgery,* vol. 128, pp. 596-599, 1993.

[10] Z. Wang, J. Nong, R. B. Shultz, Z. Zhang, T. Kim, V. J. Tom*, et al.*, "Local delivery of minocycline from metal ion-assisted self-assembled complexes promotes neuroprotection and functional recovery after spinal cord injury," *Biomaterials,* vol. 112, pp. 62-71, 2017.

[11] W. L. Fanning, D. W. Gump, and R. A. Sofferman, "Side effects of minocycline: a double-blind study," *Antimicrobial agents and chemotherapy,* vol. 11, pp. 712-717, 1977.

[12] Z. Liu, Y. Jiao, Y. Wang, C. Zhou, and Z. Zhang, "Polysaccharides-based nanoparticles as drug delivery systems," *Advanced drug delivery reviews,* vol. 60, pp. 1650-1662, 2008.

[13] L. A. Segel and M. Slemrod, "The quasi-steady-state assumption: a case study in perturbation," *SIAM review,* vol. 31, pp. 446-477, 1989.

Software

[I] MATLAB 2016, MathWorks, 2016

[II] Excel 2010, Microsoft, 2010

[III] MOPAC, Stewart Computational Chemistry

[IV] ChemDraw, PerkinElmer Informatics Desktop Software

Appendix

Solutions

Table 7: Hank's Buffered Saline Solution formulation

Adjust pH to 7.1-7.4 after dissolving		
	mg/L	**mg/mL**
CaCl2	140	0.14
KCl	400	0.4
KH2PO4	60	0.06
*MgSO4*7H2O*	200	0.2
NaCl	8000	8
*Na2HPO4*7H2O*	90.07	0.09007
NaHCO3	350	0.35

Equipment and Materials

Table 8: Equipment

Equipment	**Use**
Eppendorf Research Plus Pipettes	Accurate volume transfer
Beckman Coulter Microfuge 22R Centrifuge	Separation of particles from solution
Tecan Infinite 200 NanoQuant	Spectrometer for concentration measurements
Zetasizer Nano ZS90	Particle size and characteristics

Table 9: Materials

Material	**Source and Model Number**
Minocycline Hydrochloride	Sigma Aldrich: M9511
Dextran Sulfate	Sigma Aldrich: D8906
Magnesium Chloride	Sigma Aldrich: M9272
Agarose (SeaPlaque)	Loza: 50101